Asp174 and Asp175 as the Key Catalytic Residues of Human O-GlcNAcase by Functional Analysis of Site-Directed Mutants. Biochemistry, 45(11), 3835–3844. https://doi.org/10.1021/bi052370b

Identification of Asp[174] and Asp[175] as the Key Catalytic Residues of Human *O*-GlcNAcase by Functional Analysis of Site-Directed Mutants[†]

Naniye Çetinbaş,[‡] Matthew S. Macauley,[‡] Keith A. Stubbs, Robert Drapala, and David J. Vocadlo*

Department of Chemistry, Simon Fraser University, 8888 University Drive, Burnaby, British Columbia, Canada, V5A 1S6

Received November 20, 2005; Revised Manuscript Received January 18, 2006

ABSTRACT: *O*-GlcNAcase is a family 84 *β*-*N*-acetylglucosaminidase catalyzing the hydrolytic cleavage of *β*-*O*-linked 2-acetamido-2-deoxy-D-glycopyranose (*O*-GlcNAc) from serine and threonine residues of posttranslationally modified proteins. *O*-GlcNAcases use a double-displacement mechanism involving formation and breakdown of a transient bicyclic oxazoline intermediate. The key catalytic residues of any family 84 enzyme facilitating this reaction, however, are unknown. Two mutants of human *O*-GlcNAcase, D174A and D175A, were generated since these residues are highly conserved among family 84 glycoside hydrolases. Structure−reactivity studies of the D174A mutant enzyme reveals severely impaired catalytic activity across a broad range of substrates alongside a pH−activity profile consistent with deletion of a key catalytic residue. The D175A mutant enzyme shows a significant decrease in catalytic efficiency with substrates bearing poor leaving groups (up to 3000-fold), while for substates bearing good leading groups the difference is much smaller (7-fold). This mutant enzyme also cleaves thioglycosides with essentially the same catalytic efficiency as the wild-type enzyme. As well, addition of azide as an exogenous nucleophile increases the activity of this enzyme toward a substrate bearing an excellent leaving group. Together, these results allow unambiguous assignment of Asp[174] as the residue that polarizes the 2-acetamido group for attack on the anomeric center and Asp[175] as the residue that functions as the general acid/base catalyst. Therefore, the family 84 glycoside hydrolases use a DD catalytic pair to effect catalysis.

O-GlcNAcase, a member of the family 84 glycoside hydrolases (*1*), acts to hydrolyze 2-acetamido-2-deoxy-*β*-D-glucopyranose (*O*-GlcNAc)[1] residues from posttranslationally modified serine and threonine residues of nucleocytoplasmic proteins (*2*−*4*). Consistent with the important cellular role that this modification plays, a number of diseases have been associated with its dysregulation, including diabetes (*5*, *6*), Alzheimer (*7*−*9*), and cancer (*10*). Indeed, disruption of the gene responsible for addition (*O*GTase) or removal (*O*-GlcNAcase) of *O*-GlcNAc has been associated with diseased states (*11*, *12*). We have previously determined that, in a fashion similar to members of families 18 (*13*, *14*), 20 (*15*−*17*), and 56 (*18*) of glycoside hydrolases, *O*-GlcNAcase (*19*) uses a catalytic mechanism involving anchimeric assistance from the 2-acetamido group of the substrate. The overall reaction proceeds in two ordered steps each involving inversion of stereochemistry at the anomeric center such that the reaction proceeds with overall retention of stereochemistry (Figure 1). To effect this reaction, glycosidases from families 18, 20, and 56, which all use substrate-assisted catalysis, have evolved active sites in which two strategically positioned carboxyl residues (*13*, *15*, *16*, *18*) play key catalytic roles (*20*−*24*). In the first step catalyzed by these enzymes, the cyclization step, one carboxyl residue within the enzyme active site assists in formation of an oxazoline intermediate by polarizing the 2-acetamido group of the substrate to increase its nucleophilicity, thereby promoting attack of the carbonyl oxygen at the anomeric center. The other carboxyl group concomitantly facilitates departure of the aglycone leaving group by providing general acid catalysis. The second step, ring opening of the bicyclic oxazoline intermediate, occurs by the near microscopic reverse of the first step. During ring opening, the residue acting as the general acid catalyst in the first step now acts as a general base, promoting attack of a water molecule at the anomeric center to yield the *β*-hemiacetal product (*25*). The polarizing residue now facilitates this second step by assisting in the expulsion of the 2-acetamido group from the anomeric center.

For the families 18, 20, and 56 glycoside hydrolases that all use a catalytic mechanism involving anchimeric assistance from the 2-acetamido group of GlcNAc, the two key catalytic residues have, in each case, been identified previously by both structural and kinetic studies. Chitinases from family 18 (*13*, *14*, *24*) and hyaluronidases from family 56 (*18*, *22*)

[†] This work was supported by the Natural Sciences and Engineering Research Council of Canada (NSERC) and the Protein Engineering Centers of Excellence (PENCE). D.J.V. is supported as a Tier II Canada Research Chair. M.S.M. is supported by graduate fellowships from NSERC and the Michael Smith Foundation for Health Research (MSFHR).

* To whom correspondence should be addressed. Phone: 604-291-3530. Fax: 604-291-3765. E-mail: dvocadlo@sfu.ca.

[‡] These authors contributed equally.

[1] Abbreviations: WT, wild type; MT, mutant; GlcNAc, 2-acetamido-2-deoxy-*β*-D-glucopyranose; *O*-GlcNAc, polypeptidyl 2-acetamido-2-deoxy-*β*-D-glucopyranoside; pNP-*O*-GlcNAc, 4-nitrophenyl 2-acetamido-2-deoxy-*β*-D-glucopyranoside; pNP-*S*-GlcNAc, 4-nitrophenyl 2-acetamido-2-deoxy-1-thio-*β*-D-glucopyranoside; 3,4-DNP-GlcNAc, 3,4-dinitrophenyl GlcNAc; mNP-GlcNAc, 3-nitrophenyl GlcNAc; 3FpNP-GlcNAc, 3-fluoro-4-nitrophenyl-GlcNAc; 4-MU-GlcNAc, 4-methylumbelliferyl-GlcNAc; pClP-GlcNAc, 4-chlorophenyl-GlcNAc; pNHAcP-GlcNAc, *N*-acetyl-4-aminophenyl-GlcNAc; P-GlcNAc, phenyl-*O*-GlcNAc.

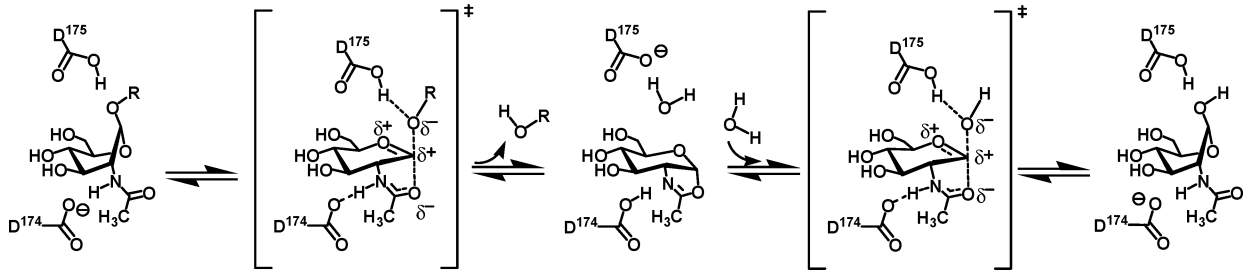

FIGURE 1: *O*-GlcNAcase uses a catalytic mechanism involving substrate-assisted catalysis. The first step of the reaction, cyclization, proceeds via attack of the 2-acetamido carbonyl oxygen on the anomeric center to form a covalent bicyclic oxazoline intermediate. This step is facilitated by polarization of the 2-acetamido moiety by an enzymic carboxyl group most likely acting as a general base catalyst. Departure of the aglycone is facilitated by general acid catalysis provided by another carboxyl group in the enzyme active site. In the second step, ring opening, the oxazoline intermediate is broken open by the general base-catalyzed attack of a water molecule on the anomeric center and general acid catalysis to the departing amide group. Both steps occur with inversion of stereochemistry at the anomeric center such that the overall reaction proceeds with net retention of stereochemistry.

use a DXE motif to effect catalysis where the aspartate operates as the polarizing residue and the glutamate serves the role of general acid/base catalyst. The family 20 glycoside hydrolases, which cleave terminal GlcNAc residues from a wide variety of glycoconjugates, employ a DE catalytic pair where the aspartate and glutamate residues are immediately adjacent to each other in sequence (*15*, *16*, *20*−*23*). Similar to the family 18 and 56 enzymes, the aspartate acts as the polarizing residue and the glutamate acts as the general acid/base catalyst. Given that we have shown the family 84 glycoside hydrolases also use a catalytic mechanism involving anchimeric assistance, we previously proposed this enzyme would also employ two key catalytic carboxyl residues (*19*). Nevertheless, the identities of these putative catalytic residues in *O*-GlcNAcase or any family 84 glycoside hydrolase remain unknown.

Human *O*-GlcNAcase is a 916-amino-acid protein with distinct N- and C-terminal domains that are apparent from sequence alignments (*26*). In one case, a region corresponding to amino acids 63−283 in the amino terminus was hypothesized to contain the catalytic glycoside hydrolase domain of *O*-GlcNAcase (*4*). Others have suggested that the C-terminal domain is essential for *O*-GlcNAcase activity (*26*−*28*). Still, other data indicate that the C-terminal domain has histone acetyl transferase activity in vitro (*29*). Nevertheless, to date no experimental data clearly indicates which domain has the molecular machinery responsible for catalyzing glycoside hydrolysis in any family 84 glycoside hydrolase.

Using a fold recognition bioinformatics approach in conjunction with modeling, Rigden et al. have predicted that family 84 glycosidases along with families 29, 44, 50, 71, 85, and 89 all have $(\alpha/\beta)_8$ TIM barrel structures (*30*). This bioinformatics study also suggested that Asp^{295} and Asp^{296} within the bacterial *Xanthomonas axonopodis* family 84 enzyme are the key catalytic residues (*30*). These residues correspond to conserved residues within the human enzyme that are found in the N-terminal domain, consistent with an earlier proposal by Hanover that this region comprises the glycosyl hydrolase domain (*4*). This contrasts with another bioinformatics study by Schultz and Pils that predicted the C-terminal domain contains *O*-GlcNAcase catalytic machinery (*31*), as well as experimental data indicating the necessity of the C-terminal domain for catalytic activity (*28*). On the basis of a hypothetical $(\alpha/\beta)_8$ TIM barrel structure of the *X. axonopodis* enzyme, a small portion of the family 84 active site containing the conserved $D^{295}D^{296}$ pair can apparently be structurally aligned with the active site of family 20 β-hexosaminidases containing a DE catalytic pair (*15*, *16*, *30*). To resolve the ambiguities between these two bioinformatics studies and to identify the key catalytic residues of *O*-GlcNAcase and by extension all family 84 glycoside hydrolases, we have subcloned the N- and C-terminal domains and have generated site-directed mutants of two highly conserved residues hypothesized by Rigden et al. to be in the glycoside hydrolase domain of human *O*-GlcNAcase (*30*) (Figure 2). Detailed kinetic studies encompassing comparative analyses of pH activity profiles, Brønsted dependence, nucleophile effects, and thioglycosidase activities of WT and mutant enzymes permit unambiguous assignment of Asp^{174} as the polarizing residue and Asp^{175} as the general acid/base catalyst.

MATERIALS AND METHODS

Reagents, Enzymes, and Bacterial Strains. All media components were obtained from Bioshops. *Pfu* DNA polymerase, deoxynucleoside triphosphates, and restriction endonucleases were obtained from Fermentas. T4 DNA ligase was purchased from New England Biolabs. *Escherichia coli* ultracompetent XL-10 Gold cells were purchased from Stratagene. *E. coli* Tuner(λDE3) cells were purchased from Novagen. HisTrap FF columns were purchased from Amersham Biosciences. DNA fragment purification and plasmid purification kits were obtained from Qiagen. Synthesis of oligonugleotide primers and DNA sequencing were performed by the Nucleic Acids and Peptide Service (NAPS) facility, University of British Columbia. The synthesis of aryl 2-acetamido-2-deoxy-β-D-glucosides is described elsewhere (*32*, *33*).

Cloning of the N- and C-Terminal Domain of Human O-GlcNAcase. Subcloning of the DNA encoding full-length human *O*-GlcNAcase into pET28a and conditions used were described previously (*32*). Similar conditions were used to subclone the N- and C-terminal domain of human *O*-GlcNAcase into the pET28a expression vector. Primers used to carry out the subcloning for the N-terminal domain were as follows: 5′-GCCGCC**CATATG**GTGCAGAAGGAGAGTCAAGCG-3′ and 5′-GCCGCC**CTCGAG***CTA*ATCTTCACTGTCAGTCATCA-3′. Primers used to carry out the subcloning of the C-terminal domain were as follows: 5′-GCCGCC**CATATG**AGTACTGTGTCCATCCAGATAAAATTAG-3′ and 5′-GCCGCC**CTCGAG***CTA*CAGGCTCCGACCAA-

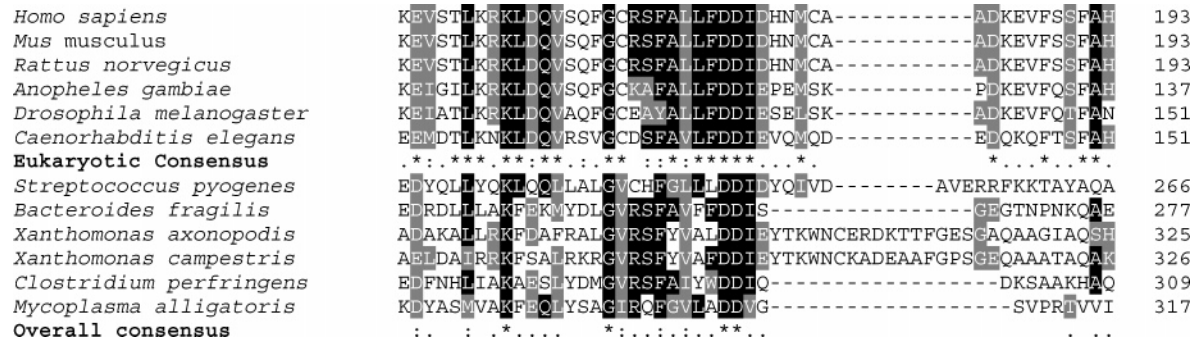

FIGURE 2: Sequence alignment of family 84 glycoside hydrolases show that Asp[174] and Asp[175] from human *O*-GlcNAcase are fully conserved. The top half of the alignment shows members of family 84 glycoside hydrolases from eukaryotes, while the bottom half shows those of prokaryotes. The data bank accession numbers are as follows: *Homo sapiens*: (GenBank identifier AF036144; *Mus musculus* (GenBank identifier AF132214); *Rattus norvegicus* (GenBank identifier AY039679); *Anaopheles gambiae* (GenBank identifier AAAB01008799); *Drosophila melanogaster* (GenBank identifier AE003734); *Caenorhabditis elegans* (GenBank identifier U28742); *Streptococcus pyogenes* (GenBank identifier AE006591); *Bacteroides fragilis* (GenBank identifier CR626927); *Xanthomonas axonopodis* (GenBank identifier AE012042); *Xanthomonas campestris* (GenBank identifier CP000050); *Clostridium perfringens* (GenBank identifier AP003185); and *Mycoplasma alligatoris* (GenBank identifier AY515698). Fully conserved (*), semi-conserved (:) and partially conserved (·) residues are shown for the eukaryotic sequences and for all sequences. The sequence alignment was carried out using the program ClustalW (*66*) and BOXSHADE.

GTATAACC-3′. Bold lettering represents the restriction sites (NdeI and XhoI), and the italics represents an inserted stop codon.

Mutagenesis of Full-Length O-GlcNAcase. The pET28a plasmid containing full-length *O*-GlcNAcase was used to create the site-directed mutants D174A and D175A. The primers used for the mutagenesis were as follows: D174A forward: 5′-GCAGATCATTTGCTTTGCTTTTTG**CA**GATATAGACCATAATATGTGTGC-3′; D174A reverse: 5′-GCACACATATTATGGTCTATATCT**GC**AAAAAGCAAAGCAAATGATCT-GC3′; D175A forward: 5′-CAGATCATTTGCTTTGCTTTTTGATG**CA**ATAGACCATAA-TATGTGTGCAGC-3′; D175A reverse: 5′-GCTGCACACATATTATGGTCTAT**TG**CATC-AAAAAGCAAAGCAAATGATCTG-3′ (mutated nucleotides are shown in bold case). Double base pair substitutions were made to reduce low levels of translational misincorporation by the ribosome during protein synthesis in the host cell. Mutagenesis conditions were described previously (*32*).

Overexpression and Purification of Proteins. All full-length proteins as well as the N-terminal domain were overexpressed and purified by Ni^{2+}-affinity chromotography as described previously (*32*). Great care was taken to avoid cross contamination by using separate nickel columns for each protein.

Kinetic Analyses. Conditions at which the Brønsted analyses and pH-dependent catalysis of *O*-GlcNAcase were carried out were described previously (*32*). Effects of adding endogenous nucleophiles on enzyme catalyzed hydrolysis of 3,4-DNP-GlcNAc were determined by following the reaction progress spectrophotometrically in a continuous assay at 37 °C using a 96-well plate (Sarstedt) and 96-well plate reader (Molecular Devices). A carefully pH adjusted solution containing 1 M sodium azide in PBS buffer (pH 7.4) was added to the appropriate amount of PBS buffer (pH 7.4) to achieve the desired final concentration of azide in the assays. The pH of the resulting solution was verified in all cases to be 7.40 ± 0.05. In addition, a parallel set of assays were carried out as described above, except sodium chloride was used to estimate changes in the rates that might arise from variation in the ionic strength of the reaction mixture.

RESULTS

Identification of the Glycoside Hydrolase Domain of O-GlcNAcase. To clearly establish which domain harbors *O*-GlcNacase activity, we generated two deletion constructs comprising amino acids 1−350 and 351−916 of human *O*-GlcNAcase. Recombinant proteins were expressed in *E. coli* and purified by Ni^{2+}-affinity chromatography. Purified proteins were tested for activity toward pNP-*O*-GlcNAc as a substrate. Only the N-terminal domain showed catalytic activity ($V_{max}/[E]_0 = 0.002$ μmol min^{-1} mg^{-1}, $K_M = 1.5$ mM, $V_{max}/[E]_0K_M = 0.0013$ μmol min^{-1} mg^{-1} mM^{-1}).

Production and Purification of Mutant Enzymes. To identify the catalytic residues of human *O*-GlcNAcase within the N-terminal domain, a completely conserved DD pair (Asp[174] and Asp[175]) found in all members of family 84 glycoside hydrolases (Figure 2) were mutated to alanine residues in the full-length protein. Successful site-directed mutagenesis was verified by DNA sequencing. The two mutant *O*-GlcNAcases as well as the WT enzyme were then overexpressed and purified by Ni^{2+}-affinity chromatography. Purity of the proteins was verified using SDS−PAGE, and it confirmed that the enzymes used in this study were >95% pure of contaminating *E. coli* proteins (see Supporting Information).

pH-Dependence Activity Profiles. Full Michaelis−Menten parameters were measured at pH values ranging from 4.5 to 9.0, in which the enzyme was stable over the assay time (30 min). Shown in Figure 3 are plots of the logarithm of the second-order rate constants ($V_{max}/[E]_0K_M$) for WT *O*-GlcNAcase and the two mutants as a function of pH. As both others and ourselves have shown previously (*3*, *32*), the pH activity profile for the WT-catalyzed hydrolysis of pNP-*O*-GlcNAc resembles a bell-shaped curve with the maximal catalytic efficiency at a pH of 6.5 (Figure 3). The hydrolysis of pNP-*O*-GlcNAc catalyzed by the D174A mutant is extremely slow; therefore, a more reactive substrate (3,4-DNP-GlcNAc) was used for determining its pH profile. Strikingly, the pH profile for the D174A mutant did not show a bell-shaped curve but rather increasing activity at lower pH values (Figure 3). Analysis of the pH profile of the D175A mutant using pNP-*O*-GlcNAc showed behavior similar to that of

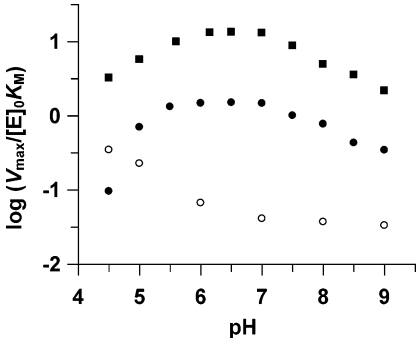

FIGURE 3: The pH activity profiles of wild-type *O*-GlcNAcase and the two mutants strongly suggests that Asp^{174} is the polarizing residue and hints at Asp^{175} being the general acid/base catalyst. The second-order rate constant for WT (■) and D175A (●) *O*-GlcNAcase catalyzed hydrolysis of pNP-*O*-GlcNAc and D174A (○) catalyzed hydrolysis of 3,4-DNP-GlcNAc as a function of pH of the reaction mixture.

the WT enzyme with the exception that the activity did not drop as much at higher pH values (Figure 3).

Brønsted Analyses. The Michaelis−Menten parameters for the enzyme-catalyzed hydrolysis of a series of substituted aryl glycosides were determined with both mutant enzymes and compared to those previously obtained with the WT enzyme (*32*) (Table 1). The resulting Brønsted plots of log(V_{max}/[E]$_0K_M$) versus pK_a of the aryl leaving group for the WT and mutant enzymes are shown in Figure 4A,B. As we described previously for WT *O*-GlcNAcase (*32*), the $\beta_{lg}(V/K)$ value is −0.11. In contrast, a $\beta_{lg}(V/K)$ value of −0.95 is obtained for the D174A mutant. When measured at pH 5.0, however, the β_{lg} value was much less negative ($\beta_{lg}(V/K) = -0.39$). For the D175A mutant enzyme, a curved plot with a defined linear region was obtained (Figure 4B). For good substrates, with pK_a values of the corresponding phenol leaving groups < 7.2, the plot unexpectedly deviates from linearity with a decreasing negative slope. For poor substrates, having phenol leaving groups with pK_a values >7.2, a steep negative slope ($\beta_{lg}(V/K) = -1.0$) is observed.

Brønsted plots relating the logarithm of the first-order rate constant (V_{max}/[E]$_0$) to the pK_a value of the corresponding phenol leaving group (Figure 4C,D) show that for WT *O*-GlcNAcase there is no dependency on the leaving group. The situation changes, however, for the mutant enzymes. For the D175A mutant, a similar pattern for plots of the first-order (Figure 4D) and second-order (Figure 4B) rate constants is obtained. With good leaving groups, there is no dependency on the leaving group ($\beta_{lg}(V) \approx 0.00$), whereas with poor leaving groups there is a clear dependency ($\beta_{lg}(V) = -0.77$). For the D174A mutant, there is also a trend but once again it is pH-dependent (Figure 4C). At pH 7.4, the slope of the Brønsted plot is steep ($\beta_{lg}(V) = -0.71$), whereas at pH 5.0 the slope is much more shallow ($\beta_{lg}(V) = -0.31$).

Competitive Nucleophile Effects. The effect of competitive nucleophiles on the rates of hydrolysis of 3,4-DNP-GlcNAc catalyzed by the WT enzyme and the two mutants was also investigated. For the WT enzyme as well as the D174A mutant, addition of 600 mM azide did not result in any rate enhancement. A greater than 5-fold increase, however, was observed for the activity of the D175A mutant. Nucleophile rescue experiments were also attempted using either β-mercaptoethanol or formate, but the results were not as striking as those seen with azide (data not shown). In addition, the azide effect is not observed when a substrate bearing a poor leaving group (mNP-GlcNAc) is used (data not shown). A more detailed kinetic analysis of the effect of azide on the D175A mutant enzyme was performed. The first- and second-order rate constants, as well as the Michaelis constants determined as a function of azide concentration for the D175A mutant, are shown in Figure 5. Both V_{max}/[E]$_0$ and K_M values increase as a function of azide concentration, with the overall result that V_{max}/[E]$_0K_M$ only slightly increases. Further, by comparison to a synthetic standard using TLC analysis, the D175A-catalyzed formation of 2-acetamido-2-deoxy-β-D-glucopyranosyl azide could be

Table 1: Kinetic Parameters for the Hydrolysis a Series of Aryl-*O*-glycosides with WT *O*-GlcNAcase and the D174A and D175A Mutants

substrate	pK_a[a]	enzyme	V_{max}/[E]$_0$[b] (μmol min^{-1} mg^{-1})	K_M[c] (mM)	V_{max}/[E]$_0K_M$ (μmol min^{-1} mg^{-1} mM^{-1})
3,4-DNP-GlcNAc	5.42	WT	2.4	0.21	12
		D174A (pH 7.4)	0.02	0.56	0.041
		D174A (pH 5.0)	0.02	0.36	0.35
		D175A	0.36	0.22	1.7
3FpNP-GlcNAc	6.42	WT	2.3	0.33	7.1
		D174A (pH 7.4)	0.003	0.38	0.0072
		D174A (pH 5.0)	0.03	0.73	0.21
		D175A	0.45	0.31	1.5
pNP-*O*-GlcNAc	7.18	WT	1.5	0.21	7.4
		D174A (pH 7.4)	0.002	1.4	0.0011
		D174A (pH 5.0)	0.01	0.46	0.071
		D175A	0.23	0.23	1.0
4-MU-GlcNAc	7.5	WT	1.2	0.2	6.2
		D174A (pH 7.4)	0.0006	1.4	0.0004
		D175A	0.05	0.2	0.24
mNP-GlcNAc	8.39	WT	2.3	0.47	5.0
		D175A	0.03	0.95	0.028
pClP-GlcNAc	9.47	WT	2.2	0.56	3.9
pNHAcP-GlcNAc	9.5	WT	3.1	0.84	3.7
P-GlcNAc	9.99	WT	2.1	0.62	3.4
		D175A	0.001	0.95	0.0012

[a] Values were determined previously (*63*−*65*). [b] Errors were between 2 and 5% except those for the D174A mutant enzyme for which the errors are between 5 and 10%. [c] Errors were between 10 and 15% except those for the D174A mutant enzyme for which the errors are between 10 and 25%.

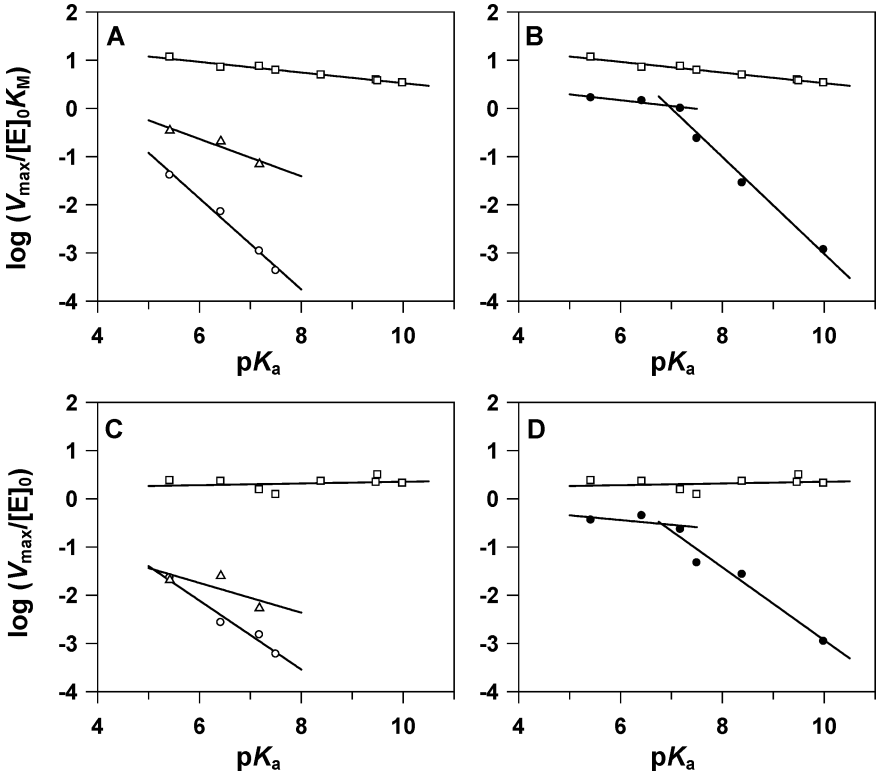

FIGURE 4: Brønsted analyses of the WT and mutant *O*-GlcNAcase catalyzed hydrolysis of a series of substrates bearing substituted aryl leaving groups. (A and B) Brønsted plots of the logarithm of the second-order rate constants for the (A) D174A mutant at pH 7.4 (○) and pH 5.0 (△), and (B) the D175A mutant (●) compared to those for the WT enzyme (□). (C and D) Brønsted plots of the logarithm of the first-order rate constant for (C) the D174A mutant at pH 7.4 (○) and pH 5.0 (△), and (D) the D175A mutant (●) compared to those for the WT enzyme (□). Data for the WT enzyme were taken from ref 32.

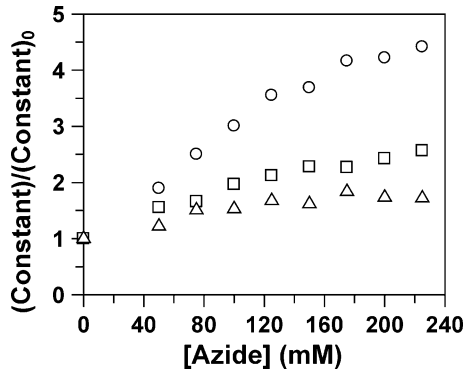

FIGURE 5: Adding azide as an exogenous nucleophile partially rescues the activity of the D175A mutant toward 3,4-DNP-GlcNAc. The first-order rate constants, V_{max}/[E]$_0$ (○), Michaelis constants, K_M (□), and second-order rate constants, V_{max}/[E]$_0$ K_M (△), for the D175A mutant plotted as a function of azide concentration. All values are corrected for the effect of salt concentration on the activity of the D175A mutant enzyme.

observed when azide was included in the reaction (Supporting Information).

Cleavage of an S-Glycoside. Previously, we have shown that *O*-GlcNAcase has an unusual property among glycosidases of being able to catalyze the hydrolysis of *S*-glycosides with reasonable catalytic efficiency (*32*). The enzyme was shown to effect cleavage of *S*-glycosides without general acid catalysis (*32*). Accordingly, the two mutant enzymes were tested for thioglycosidase activity toward pNP-*S*-GlcNAc, and the rate constants governing hydrolysis were compared to those obtained for pNP-*O*-GlcNAc. The D175A mutant shows significant activity toward pNP-*S*-GlcNAc that is similar to its activity toward pNP-*O*-GlcNAc (Table 2). On the other hand, the D174A mutant shows essentially no activity toward pNP-*S*-GlcNAc.

DISCUSSION

Family 84 glycoside hydrolases cleave the glycosidic linkage of *N*-acetylglucosaminides by a two-step catalytic mechanism that likely involves two key catalytic residues (*19*) (Figure 1). In this study, we sought to determine the domain of *O*-GlcNAcase that contains the glycoside hydrolase domain as well as identify the two important residues by determining the kinetic consequences of deleting these catalytic groups. Conflicting suggestions in the literature contend whether the domain within *O*-GlcNAcase bearing *N*-acetylglucosaminidase activity resides in the either the N- (*4, 29, 30*) or the C-terminus (*26*−*28, 31*). We find that only the N-terminal domain (amino acids 1−350) has glycoside hydrolase activity. Nevertheless, its activity was dramatically lower (≈1000-fold) than that of full-length enzyme. We speculate that this decreased activity may be a consequence of either a structural perturbation in the N-terminal domain stemming from absence of the C-terminal domain or that the C-terminal may play some role in catalysis. Regardless, this finding supports the prediction of Rigden et al. (*30*) and disagrees with the predictions of Schultz and Pils (*31*). Furthermore, these findings are consistent with the absence of the C-terminal domain in prokaryotic family 84 glycoside hydrolases. We therefore centered our attention on the prediction by Rigden et al, which used a fold recognition approach in conjunction with modeling to postulate a DD pair within the N-terminal domain of family 84 glycoside hydrolases to be the two essential catalytic residues (*30*).

Table 2: The D175A Mutant of Human *O*-GlcNAcase Catalyzes the Cleavage of an *S*-Glycoside with Comparable Catalytic Efficiency as an *O*-Glycoside

enzyme	$(V_{max}[E]_o^{-1}K_M^{-1})_O$ (μmol min^{-1} mg^{-1} mM^{-1})	$(V_{max}[E]_o^{-1}K_M^{-1})_S$ (μmol min^{-1} mg^{-1} mM^{-1})	$(V_{max}[E]_o^{-1}K_M^{-1})_S/(V_{max}[E]_o^{-1}K_M^{-1})_O$	$(V_{max}[E]_o^{-1}K_M^{-1})_{S(MT)}/(V_{max}[E]_o^{-1}K_M^{-1})_{S(WT)}$
WT	7.4	0.31	0.041	N.A.[b]
D174A	0.0011	N.A.[a]	N.A.[b]	N.A.[b]
D175A	1.0	0.46	0.45	1.5

[a] No detectable activity. [b] Not applicable.

The two predicted aspartate residues correspond to Asp[174] and Asp[175] of human *O*-GlcNAcase. Indeed, these residues are completely conserved throughout all predicted members of family 84 glycoside hydrolases (Figure 2). Accordingly, D174A and D175A mutants were prepared of full-length human *O*-GlcNAcase where the carboxyl group was deleted by replacing each aspartate with the nonionizable amino acid alanine. The consequences of these mutations were determined by obtaining the kinetic parameters for these mutant enzymes acting on a range of different substrates and comparing them to those obtained for the WT enzyme.

Preliminary assays of the two mutant enzymes using pNP-*O*-GlcNAc as a substrate revealed that the catalytic efficiency of both mutants were compromised (Table 1). The D174A mutant, in particular, showed a dramatic 7000-fold decrease in its second-order rate constant ($V_{max}/[E]_0K_M$) as compared to the WT enzyme. The D175A mutant, however, showed only a modest 7-fold decrease. Encouraged by our preliminary results, we decided to study the pH activity profiles as well as to carry out detailed functional analyses of both mutant enzymes.

Glycosidases typically exhibit bell-shaped pH profiles reflecting the ionizations of two important active site carboxyl groups (*34*, *35*). Deletion of one of these carboxyl groups often results in the disappearance of one of the corresponding limbs in the profile, leaving an asymmetric pH profile stemming from titration of the remaining residue (*20*, *34*, *36*−*38*). As reported previously, *O*-GlcNAcase exhibits a bell-shaped pH profile showing maximal activity at a pH value of 6.5 (*3*, *26*, *32*, *39*). The kinetic pK_a values of the two critical catalytic residues appear to be approximately 5.0 and 7.5 (Figure 3). Most likely, the appropriate ionization state of the enzyme to initiate the catalytic cycle is for the acid/base catalytic residue to be in its protonated form and the polarizing residue to be in its deprotonated form (Figure 1). Accordingly, the acidic limb likely stems from ionization of the polarizing residue, while the basic limb stems from ionization of the general acid/base catalytic residue.

Analysis of pH profiles of mutant enzymes in which the key carboxyl groups have been deleted by site-directed mutagenesis can, however, be complicated by the altered electrostatic environment within the active site, which can affect the microscopic pK_a value of the remaining catalytic side chain. Indeed, in our study the D174A mutant displayed only the basic limb shifted dramatically to lower pH, showing increasing catalytic efficiency at lower pH values (Figure 3). Accordingly, the remaining titratable group most likely represents the general acid/base catalytic residue and Asp[174] is therefore a candidate to be the polarizing residue. Such an assignment for this residue (Asp[174]) is entirely consistent with the deleterious effect on catalytic efficiency of mutating the polarizing residue of the family 20 human β-hexosaminidase (*20*) and a bacterial homologue from *Streptomyces plicatus* (*21*). Interestingly, the apparent kinetic pK_a value of the general acid/base catalytic residue in the D174A mutant decreases by at least 2.5 units as compared to the WT enzyme. This observation is consistent with deletion of a negative charge within the vicinity of the acid/base residue. Shifts in the pK_a values of ionizing groups within the active site of other glycosidases have been observed previously in several cases (*20*, *37*, *40*, *41*). The pH profile of the D175A mutant was more ambiguous. Nevertheless, the observation that the basic limb is attenuated at high pH suggests that Asp[175] may be the general acid/base catalytic residue. The basis for the unexpected decrease in activity at higher pH values for this mutant is unknown but may stem from ionization of another group within the enzyme active site.

In addition to analysis of pH profiles of mutant enzymes, Brønsted analyses of the enzyme-catalyzed cleavage of substrates bearing different leaving groups can be a powerful tool for identification of the acid/base catalyst of glycosidases (*34*). Replacement of the acid/base catalytic residue with a nonionizable residue should substantially reduce the catalytic efficiency of the mutant enzyme toward substrates bearing poor leaving groups but should have a less pronounced effect for substrates bearing good leaving groups that do not benefit significantly from general acid catalysis. These effects are a consequence of the structure of the transition state. For mutants in which the general acid/base catalytic group has been deleted, there is considerable negative charge development on the glycosidic oxygen since proton donation is not possible. The net result is that markedly negative $\beta_{lg}(V/K)$ values of ≈ -1.0 are expected for such mutant enzymes (*34*). For WT enzymes that are efficient at proton donation and accordingly have $\beta_{lg}(V/K)$ values that are small and negative there is a dramatic and diagnostic difference between the WT and corresponding general acid/base catalytic mutants (*34*, *37*, *41*−*43*). Indeed, such a case holds for the D175A mutant *O*-GlcNAcase: the Brønsted plot of the logarithm of the second-order rate constant shows a $\beta_{lg}(V/K)$ value of -1.0 for substrates bearing leaving groups with pK_a values greater than 7.2 (Figure 4B). This value is in marked contrast to the $\beta_{lg}(V/K)$ value of -0.11 that we previously reported for the WT enzyme (*32*). For substrates bearing leaving groups with pK_a values less than 7.2, however, deviation from a linear correlation occurs. As previously suggested for other enzymes (*41*, *44*), this break from linearity likely arises from the first step becoming reversible as the pK_a value of the leaving group decreases. A possible explanation is that the rate of internal return of the liberated phenol to reform the substrate competes effectively with diffusion of the phenol from the enzyme active site. Under such conditions, the cyclization step

becomes reversible, and accordingly the ring-opening step influences the second-order rate constant since this parameter is a reflection of first *irreversible* chemical step in a reaction mechanism. Brønsted plots showing such curvature have been obtained for a range of WT glycosidases. For example, those from families 1 (*45*−*47*), 3 (*44*, *48*), 11 (*49*), and 39 (*50*) all show such behavior. Regardless, these data strongly supports assignment of Asp^{175} as the general acid/base catalyst, consistent with the tentative assignment based on the pH profile as described above.

For the D174A mutant enzyme, initial studies at pH 7.4 revealed a similar scenario as seen for the D175A mutant with a $\beta_{lg}(V/K)$ value of −0.95 (Figure 4A). The data from the pH profile of this mutant indicates, however, that the remaining catalytic residue, presumably the putative general acid/base catalytic residue Asp^{175}, would not be in the optimal ionization state to effect catalysis at pH 7.4. Therefore, the studies were repeated at pH 5.0. Gratifyingly, the slope decreased significantly ($\beta_{lg}(V/K) = -0.39$), suggesting that general acid/base catalysis was at least partially operative for the D174A mutant enzyme at this pH value.

The Brønsted analyses of the logarithm of the first-order rate constants also reveal several interesting features. First, for WT *O*-GlcNAcase, there is no dependency on leaving group ability ($\beta_{lg}(V) \approx 0.0$) as defined by the p$K_a$ value of the phenol leaving group (Figure 4C). The absence of any dependency on the leaving group ability strongly indicates that the ring-opening step is rate-determining for the WT enzyme. Interestingly, similar behavior was recently shown for the family 20 β-hexosaminidase from *Streptomyces plicatus* (*44*). For the D175A mutant *O*-GlcNAcase, a steep negative slope ($\beta_{lg}(V) = -0.77$) is observed for substrates having poor leaving groups with pK_a values greater than 7.2, indicating that the rate-limiting step for these substrates has changed to the cyclization step. Conversely, for substrates with good leaving groups the $\beta_{lg}(V)$ value ≈ 0.0 (Figure 4D), indicating that for these substrates the ring-opening step is rate-determining, as is found for all substrates with the WT enzyme. These observations are consistent with the expectation that substrates bearing very good leaving groups cannot benefit from acid catalysis, and only when the leaving group is poor does general acid catalysis play an important role. For the D174A mutant assayed at pH 7.4, the rate-determining step is the cyclization step as evidenced by the steep negative slope ($\beta_{lg}(V) = -0.72$) (Figure 4C). At pH 5, however, the β_{lg} value appears to still have, at least, a moderately large negative value ($\beta_{lg}(V) = -0.31$), indicating that the cyclization step is rate-determining with this mutant at both pH values. These observations are consistent with the view that Asp^{174} plays the critical role of promoting the cyclization step by polarizing the 2-acetamido group for attack on the anomeric center.

Together, the Brønsted analyses and pH profiles of the D175A mutant provide good evidence for Asp^{175} being the general acid/base catalyst. To further support this hypothesis, the method of nucleophile rescue was used. This method is among the most reliable approaches for identifying the general acid/base catalytic residue of glycosidases and has been used for identifying the general acid/base catalytic residue of several β-retaining glycosidases that proceed via a covalent glycosyl-enzyme intermediate (*34*, *36*−*38*, *41*, *51*, *52*). Nevertheless, this approach has not been applied to enzymes using a catalytic mechanism involving substrate-assisted catalysis. The basis for this strategy is that general acid catalysis is no longer operational for glycosidases in which the acid/base residue has been mutated (*34*). Further, in the ring-opening step of the reaction catalyzed by *O*-GlcNAcase, water is activated by the same residue that acted as the general acid catalyst in the cyclization step (Figure 1). Consequently, when using a good substrate bearing an excellent leaving group that does not benefit from general acid catalysis, the general acid/base catalytic residue facilitates the overall reaction *only* by acting as a general base to promote attack of a water molecule in the ring-opening step. So, on addition of an exogenous nucleophile to a reaction mixture containing the mutant enzyme, a rate acceleration is often seen because the nucleophile can intercept the intermediate, obviating the need for the general acid/base residue. The kinetic consequences of adding an exogenous nucleophile is often an increase in k_{cat} values for the acid/base mutant enzyme as well as an increase in K_M values due to a change in the rate-limiting step of the reaction from the second to first step (*37*, *38*, *41*, *48*, *52*). The net result is a minimal change in the second-order rate constant for the reaction, which is consistent with the expectation that the exogenous nucleophile would have no effect on the first step of the reaction. Consistent with these expectations, we observe that increasing the concentration of azide in the reaction mixture results in an almost 5-fold increase in the value of $V_{max}/[E]_0$ and an almost 3-fold increase in the K_M value of the D175A mutant enzyme. This 5-fold increase in $V_{max}/[E]_0$ is close to the expected limit, which must be 6-fold since this is the difference between the first-order rate constants of the WT and D175A mutant enzyme catalyzed hydrolysis of 3,4-DNP-GlcNAc. As well, $V_{max}/[E]_0K_M$ remained relatively unchanged over the range of azide concentrations tested (Figure 5). Significantly, no considerable change in the kinetic parameters of WT and the D174A mutant enzyme were observed over a wide range of azide concentrations that could not be accounted for by changes in ionic strength of the reaction mixture. Further, analysis of the reaction mixture containing the D175A mutant enzyme incubated in the presence of azide and 3,4-DNP-GlcNAc reveals the formation of a 2-acetamido-2-deoxy-β-D-glycopyranosyl azide product. These azide effects therefore provide further support for the assignment of Asp^{175} as the general acid/base catalytic residue.

A key final piece of evidence supporting the identity of the general acid/base catalytic residue as Asp^{175} was obtained by assaying the catalytic efficiency of the WT and mutant *O*-GlcNAcases toward a thioglycoside. We recently showed that *O*-GlcNAcase cleaves thioglycosides without general acid catalysis (*32*). As in the nonenzymatic breakdown of *O*,*S*-thioacetals (*53*−*55*), it was shown that the *O*-GlcNAcase catalyzed hydrolysis of *S*-glycosides benefits little, if at all, from general acid catalysis to facilitate departure of the leaving group. We therefore speculated that a mutant *O*-GlcNAcase in which the general acid/base catalytic group has been deleted should have two unique properties that may help us distinguish it. First, if Asp^{175} is indeed the general acid/base catalytic residue, nearly identical rates of cleavage of a *S*-glycoside should be observed for both the WT and D175A mutant enzymes. Second, the D175A mutant should have comparable catalytic efficiencies toward both pNP-*S*-

GlcNAc and pNP-*O*-GlcNAc. Consistent with our expectations, not only did the D175A mutant cleave pNP-*S*-GlcNAc with comparable catalytic efficiency as the WT enzyme, but its second-order rate constant was approximately 2-fold higher (Table 2). Given that sulfur is a larger atom than oxygen and likely departs from the enzyme active site as an anion due to its inability to significantly benefit from general acid catalysis, it is not entirely surprisingly that replacement of the aspartate side chain with that of the less bulky and polar alanine residue results in a slight 2-fold increase in catalytic efficiency. Support for this view comes from studies on the only other unambiguously identified *S*-glycosidases known as myrosinases. Structural and functional studies of these β-retaining glycosidases clearly show that the general acid/base catalytic residue normally present in closely related glycosidases employing a two-step double-displacement mechanism has been replaced by a glutamine (*56*, *57*). Also consistent with our expectations, the D175A mutant enzyme shows only a small 2-fold difference in catalytic efficiency toward pNP-*S*-GlcNAc relative to pNP-*O*-GlcNAc (Table 2). This small difference is in marked contrast to the approximate 20-fold difference observed for the WT enzyme. Interestingly, the D174A mutant shows virtually no catalytic activity toward pNP-*S*-GlcNAc. This last result is consistent with our previous observation that nucleophilic participation by the 2-acetamido group of the substrate is more important for *O*-GlcNAcase catalyzed hydrolysis of *S*-glycosides than *O*-glycosides (*32*).

Together, all of these results provide conclusive experimental data that Asp^{174} acts as the catalytic residue that polarizes the 2-acetamido group of the substrate and that Asp^{175} acts as the general acid/base catalyst. Our previous studies showed that the *O*-GlcNAcase catalyzed reaction proceeds via highly dissociative transition states as determined by very large α-deuterium kinetic isotope effects measured for the hydrolysis of pNP-*O*-GlcNAc ($k_H/k_D = 1.14 \pm 0.02$) (*32*). The very small negative $\beta_{lg}(V/K)$ value measured for the WT *O*-GlcNAcase indicates very little negative charge accumulates on the glycosidic oxygen in the transition state. The net consequence of these two results strongly suggests that proton transfer by Asp^{175} to the departing aglycone must be significantly advanced in the first transition state. Furthermore, we have shown that for substrates that do not benefit from acid catalysis, the 2-acetamido group of the substrate participates as a nucleophile to a greater extent (*32*). We propose that Asp^{174} most likely functions as a general acid/base catalyst and not simply to stabilize an oxazolinium ion intermediate by Coulombic interactions. Therefore, in the first step, this residue would act as a general base, facilitating attack of the carbonyl oxygen of the amide moiety. Proton transfer from the amide group to this residue is likely complete on reaching the intermediate, which is therefore most likely an oxazoline and not an oxazolinium ion (Figure 1). This hypothesis is consistent with the dramatic change in pK_a of the protonated nitrogen as the subtrate structure changes from an amide to an oxazoline. Indeed, in solution, the pK_a of the amide must be fairly close to 15, while that of the oxazolinium ion must be *significantly* less than the value of 5.5 reported for 2-methyl-Δ^2-oxazoline (*58*). The kinetic pK_a value that we measure for the Asp^{174} residue is approximately 5.0, entirely consistent with its likely role as a general base catalyst. In the second step then, this same residue is in the correct protonation state to act as a general acid to transfer a proton to the departing amide group and thereby facilitate ring opening of the oxazoline intermediate. Such a mechanism involving two concomitant proton transfers may be operative in the other families of enzymes using anchimeric assistance. Interestingly, such a two-proton-transfer mechanism was first proposed for hen egg white lysozyme over 40 years ago (*59*). In the case of lysozyme, however, such a mechanism does not hold since it has recently been shown that lysozyme uses an enzymic nucleophile and proceeds through a covalent glycosyl enzyme intermediate (*60*).

This study also provides conclusive experimental evidence indicating that the N-terminal domain of human *O*-GlcNAcase contains the catalytic machinery responsible for glycoside hydrolysis, supporting previous suggestions (*4*, *29*, *30*). A structure of a family 84 glycosidase will be most valuable in gaining insight into the molecular architecture of the active site of this important class of enzymes and would provide a structural rationale for some of the effects observed here.

CONCLUSION

In summary, we show for the first time that members of the family 84 glycoside hydrolases employ a catalytic mechanism involving a DD catalytic unit. This is in marked contrast to glycoside hydrolases using anchimeric assistance from families 18 and 56 that use a DXE motif (*13*, *18*, *22*) and those from family 20 that use a DE pair (*15*, *16*, *20*−*23*). Interestingly, the catalytic motif is related to the position of the bond being cleaved. For instance, in families 18 and 56, which hydrolyze endoglycosidic bonds, the catalytic motifs are identical, having one amino acid between the two catalytic residues. This motif is distinct however from that found for enzymes from families 20 and 84, which hydrolyze exoglycosidic bonds and do not have an intervening residue. Furthermore, family 84 glycoside hydrolases are the first family of glycoside hydrolases, using anchimeric assistance, that do not use a glutamate as the general acid/base catalytic residue but rather use an aspartate residue. Whether there is a mechanistic rationale for the existence of three different sets of catalytic machinery giving rise to the same overall catalytic mechanisms in four distinct families of glycoside hydrolases remains unknown.

With the large number of diseases associated with the *O*-GlcNAc posttranslational modification, a key question remaining in many cases is the degree to which this modification is involved in the etiology of these illnesses. Artificially disrupting the natural levels of *O*-GlcNAc can provide insight to these questions. The levels of *O*-GlcNAc can be influenced within a cellular environment by addition of potent inhibitors of *O*-GlcNAcase (*19*, *61*) that results in increased *O*-GlcNAc levels. Alternatively, transfection of cells with either plasma-borne *O*-GlcNAcase (*28*) or an *O*-GlcNAcase-expressing adenovirus (*62*) are viable options for diminishing levels of *O*-GlcNAc. We speculate that using the catalytically impaired D174A or a D174A/D175A double mutant of *O*-GlcNAcase in transfections would be useful in functional studies to control for histone acetylase activity (*29*) or any additional, as yet undiscovered, roles that this large protein may play in the cellular environment.

ACKNOWLEDGMENT

We wish to thank A.J. Bennet and B.M. Pinto for access to equipment.

NOTE ADDED AFTER ASAP PUBLICATION

An earlier version of this paper posted ASAP on the web on February 24, 2006, contained an error in the double mutant name in the fifth to last line of the Conclusion. The name (D174A/D175A) has been corrected in this new version reposted February 24, 2006.

SUPPORTING INFORMATION AVAILABLE

A table of kinetic parameters used in the assays and SDS−PAGE indicating the level of purity of the WT and mutant enzymes used in this study as well as TLC analyses showing formation of GlcNAc-azide. This material is available free of charge via the Internet at http://pubs.acs.org.

REFERENCES

1. Henrissat, B., and Bairoch, A. (1996) Updating the sequence-based classification of glycosyl hydrolases, *Biochem. J. 316*, 695−696.
2. Wells, L., Vosseller, K., and Hart, G. W. (2001) Glycosylation of nucleocytoplasmic proteins: signal transduction and *O*-GlcNAc, *Science 291*, 2376−2378.
3. Dong, D. L., and Hart, G. W. (1994) Purification and characterization of an *O*-GlcNAc selective *N*-acetyl-β-D-glucosaminidase from rat spleen cytosol, *J. Biol. Chem. 269*, 19321−19330.
4. Hanover, J. A. (2001) Glycan-dependent signaling: O-linked *N*-acetylglucosamine, *FASEB J. 15*, 1865−1876.
5. Vosseller, K., Wells, L., Lane, M. D., and Hart, G. W. (2002) Elevated nucleocytoplasmic glycosylation by *O*-GlcNAc results in insulin resistance associated with defects in Akt activation in 3T3-L1 adipocytes, *Proc. Natl. Acad. Sci. U.S.A. 99*, 5313−5318.
6. McClain, D. A., Lubas, W. A., Cooksey, R. C., Hazel, M., Parker, G. J., Love, D. C., and Hanover, J. A. (2002) Altered glycan-dependent signaling induces insulin resistance and hyperleptinemia, *Proc. Natl. Acad. Sci. U.S.A. 99*, 10695−10699.
7. Griffith, L. S., and Schmitz, B. (1995) O-linked *N*-acetylglucosamine is upregulated in Alzheimer brains, *Biochem. Biophys. Res. Commun. 213*, 424−431.
8. Yao, P. J., and Coleman, P. D. (1998) Reduction of O-linked *N*-acetylglucosamine-modified assembly protein-3 in Alzheimer's disease, *J. Neurosci. 18*, 2399−2411.
9. Liu, F., Iqbal, K., Grundke-Iqbal, I., Hart, G. W., and Gong, C. X. (2004) *O*-GlcNAcylation regulates phosphorylation of tau: a mechanism involved in Alzheimer's disease, *Proc. Natl. Acad. Sci. U.S.A. 101*, 10804−10809.
10. Chou, T. Y., and Hart, G. W. (2001) O-linked *N*-acetylglucosamine and cancer: messages from the glycosylation of c-Myc, *Adv. Exp. Med. Biol. 491*, 413−418.
11. Hanover, J. A., Forsythe, M. E., Hennessey, P. T., Brodigan, T. M., Love, D. C., Ashwell, G., and Krause, M. (2005) A *Caenorhabditis elegans* model of insulin resistance: altered macronutrient storage and dauer formation in an OGT-1 knockout, *Proc. Natl. Acad. Sci. U.S.A. 102*, 11266−11271.
12. Lehman, D. M., Fu, D. J., Freeman, A. B., Hunt, K. J., Leach, R. J., Johnson-Pais, T., Hamlington, J., Dyer, T. D., Arya, R., Abboud, H., Goring, H. H., Duggirala, R., Blangero, J., Konrad, R. J., and Stern, M. P. (2005) A single nucleotide polymorphism in MGEA5 encoding *O*-GlcNAc-selective *N*-acetyl-β-D-glucosaminidase is associated with type 2 diabetes in Mexican Americans, *Diabetes 54*, 1214−1221.
13. van Aalten, D. M., Komander, D., Synstad, B., Gaseidnes, S., Peter, M. G., and Eijsink, V. G. (2001) Structural insights into the catalytic mechanism of a family 18 exo-chitinase, *Proc. Natl. Acad. Sci. U.S.A. 98*, 8979−8984.
14. Tews, I., vanScheltinga, A. C. T., Perrakis, A., Wilson, K. S., and Dijkstra, B. W. (1997) Substrate-assisted catalysis unifies two families of chitinolytic enzymes, *J. Am. Chem. Soc. 119*, 7954−7959.
15. Tews, I., Perrakis, A., Oppenheim, A., Dauter, Z., Wilson, K. S., and Vorgias, C. E. (1996) Bacterial chitobiase structure provides insight into catalytic mechanism and the basis of Tay-Sachs disease, *Nat. Struct. Biol. 3*, 638−648.
16. Mark, B. L., Vocadlo, D. J., Knapp, S., Triggs-Raine, B. L., Withers, S. G., and James, M. N. (2001) Crystallographic evidence for substrate-assisted catalysis in a bacterial β-hexosaminidase, *J. Biol. Chem. 276*, 10330−10337.
17. Knapp, S., Vocadlo, D., Gao, Z. N., Kirk, B., Lou, J. P., and Withers, S. G. (1996) NAG-thiazoline, an *N*-acetyl-β-hexosaminidase inhibitor that implicates acetamido participation, *J. Am. Chem. Soc. 118*, 6804−6805.
18. Markovic-Housley, Z., Miglierini, G., Soldatova, L., Rizkallah, P. J., Muller, U., and Schirmer, T. (2000) Crystal structure of hyaluronidase, a major allergen of bee venom, *Structure 8*, 1025−1035.
19. Macauley, M. S., Whitworth, G. E., Debowski, A. W., Chin, D., and Vocadlo, D. J. (2005) *O*-GlcNAcase uses substrate-assisted catalysis: kinetic analysis and development of highly selective mechanism-inspired inhibitors, *J. Biol. Chem. 280*, 25313−25322.
20. Hou, Y., Vocadlo, D. J., Leung, A., Withers, S. G., and Mahuran, D. (2001) Characterization of the Glu and Asp residues in the active site of human β-hexosaminidase B, *Biochemistry 40*, 2201−2209.
21. Williams, S. J., Mark, B. L., Vocadlo, D. J., James, M. N., and Withers, S. G. (2002) Aspartate 313 in the Streptomyces plicatus hexosaminidase plays a critical role in substrate-assisted catalysis by orienting the 2-acetamido group and stabilizing the transition state, *J. Biol. Chem. 277*, 40055−40065.
22. Arming, S., Strobl, B., Wechselberger, C., and Kreil, G. (1997) In vitro mutagenesis of PH-20 hyaluronidase from human sperm, *Eur. J. Biochem. 247*, 810−814.
23. Prag, G., Papanikolau, Y., Tavlas, G., Vorgias, C. E., Petratos, K., and Oppenheim, A. B. (2000) Structures of chitobiase mutants complexed with the substrate di-*N*-acetyl-D-glucosamine: the catalytic role of the conserved acidic pair, aspartate 539 and glutamate 540, *J. Mol. Biol. 300*, 611−617.
24. Lu, Y., Zen, K. C., Muthukrishnan, S., and Kramer, K. J. (2002) Site-directed mutagenesis and functional analysis of active site acidic amino acid residues D142, D144 and E146 in *Manduca sexta* (tobacco hornworm) Chitinase, *Insect Biochem. Mol. Biol. 32*, 1369−1382.
25. Mark, B. L., and James, M. N. G. (2002) Anchimeric assistance in hexosaminidases, *Can. J. Chem. 80*, 1064−1074.
26. Gao, Y., Wells, L., Comer, F. I., Parker, G. J., and Hart, G. W. (2001) Dynamic O-glycosylation of nuclear and cytosolic proteins: cloning and characterization of a neutral, cytosolic β-*N*-acetylglucosaminidase from human brain, *J. Biol. Chem. 276*, 9838−9845.
27. Zachara, N. E., and Hart, G. W. (2004) *O*-GlcNAc a sensor of cellular state: the role of nucleocytoplasmic glycosylation in modulating cellular function in response to nutrition and stress, *Biochim. Biophys. Acta 1673*, 13−28.
28. Wells, L., Gao, Y., Mahoney, J. A., Vosseller, K., Chen, C., Rosen, A., and Hart, G. W. (2002) Dynamic O-glycosylation of nuclear and cytosolic proteins: further characterization of the nucleocytoplasmic β-*N*-acetylglucosaminidase, *O*-GlcNAcase, *J. Biol. Chem. 277*, 1755−1761.
29. Toleman, C., Paterson, A. J., Whisenhunt, T. R., and Kudlow, J. E. (2004) Characterization of the histone acetyltransferase (HAT) domain of a bifunctional protein with activable *O*-GlcNAcase and HAT activities, *J. Biol. Chem. 279*, 53665−53673.
30. Rigden, D. J., Jedrzejas, M. J., and de Mello, L. V. (2003) Identification and analysis of catalytic TIM barrel domains in seven further glycoside hydrolase families, *FEBS Lett. 544*, 103−111.
31. Schultz, J., and Pils, B. (2002) Prediction of structure and functional residues for *O*-GlcNAcase, a divergent homologue of acetyltransferases, *FEBS Lett. 529*, 179−182.
32. Macauley, M. S., Stubbs, K. A., and Vocadlo, D. J. (2005) *O*-GlcNAcase catalyzes cleavage of thioglycosides without general acid catalysis, *J. Am. Chem. Soc. 127*, 17202−17203.
33. Stubbs, K. A., Macauley, M. S., and Vocadlo, D. J. (2006) A highly concise preparation of O-deacetylated arylthioglycosides of *N*-acetylglucosamine from 2-acetamido 3,4,6-tri-O-acetyl-2-deoxy-α-D-glucopyranosyl chloride and aryl thiols or disulfides, *Carbohydr. Res.*, published online February 10, 2006. http://dx.doi.org/10.1016/j.carres.2005.12.009.
34. Ly, H. D., and Withers, S. G. (1999) Mutagenesis of glycosidases, *Annu. Rev. Biochem. 68*, 487−522.

35. Davies, G. J., Sinnott, M. L., and Withers, S. G. (1998) *Comprehensive Biological Catalysis: A Mechanistic Reference*, Academic Press, San Diego.
36. MacLeod, A. M., Tull, D., Rupitz, K., Warren, R. A., and Withers, S. G. (1996) Mechanistic consequences of mutation of active site carboxylates in a retaining β-1,4-glycanase from *Cellulomonas fimi*, *Biochemistry 35*, 13165−13172.
37. Bravman, T., Mechaly, A., Shulami, S., Belakhov, V., Baasov, T., Shoham, G., and Shoham, Y. (2001) Glutamic acid 160 is the acid−base catalyst of β-xylosidase from *Bacillus stearothermophilus* T-6: a family 39 glycoside hydrolase, *FEBS Lett. 495*, 115−119.
38. Bravman, T., Belakhov, V., Solomon, D., Shoham, G., Henrissat, B., Baasov, T., and Shoham, Y. (2003) Identification of the catalytic residues in family 52 glycoside hydrolase, a β-xylosidase from Geobacillus stearothermophilus T-6, *J. Biol. Chem. 278*, 26742−26749.
39. Penton, E., Poenaru, L., and Dreyfus, J. C. (1975) Hexosaminidase-C in Tay-Sachs and Sandhoff disease, *Biochim. Biophys. Acta 391*, 162−169.
40. McIntosh, L. P., Hand, G., Johnson, P. E., Joshi, M. D., Korner, M., Plesniak, L. A., Ziser, L., Wakarchuk, W. W., and Withers, S. G. (1996) The pK_a of the general acid/base carboxyl group of a glycosidase cycles during catalysis: a ^{13}C NMR study of bacillus circulans xylanase, *Biochemistry 35*, 9958−9966.
41. Vocadlo, D. J., Wicki, J., Rupitz, K., and Withers, S. G. (2002) A case for reverse protonation: identification of Glu160 as an acid/base catalyst in *Thermoanaerobacterium saccharolyticum* β-xylosidase and detailed kinetic analysis of a site-directed mutant, *Biochemistry 41*, 9736−9746.
42. MacLeod, A. M., Lindhorst, T., Withers, S. G., and Warren, R. A. (1994) The acid/base catalyst in the exoglucanase/xylanase from *Cellulomonas fimi* is glutamic acid 127: evidence from detailed kinetic studies of mutants, *Biochemistry 33*, 6371−6376.
43. Watson, J. N., Newstead, S., Dookhun, V., Taylor, G., and Bennet, A. J. (2004) Contribution of the active site aspartic acid to catalysis in the bacterial neuraminidase from *Micromonospora viridifaciens*, *FEBS Lett. 577*, 265−269.
44. Vocadlo, D. J., and Withers, S. G. (2005) Detailed comparative analysis of the catalytic mechanisms of β-*N*-acetylglucosaminidases from Families 3 and 20 of glycoside hydrolases, *Biochemistry 44*, 12809−12818.
45. Dale, M. P., Kopfler, W. P., Chait, I., and Byers, L. D. (1986) β-glucosidase: substrate, solvent, and viscosity variation as probes of the rate-limiting steps, *Biochemistry 25*, 2522−2529.
46. Kempton, J. B., and Withers, S. G. (1992) Mechanism of Agrobacterium β-glucosidase: kinetic studies, *Biochemistry 31*, 9961−9969.
47. Bauer, M. W., and Kelly, R. M. (1998) The family 1 B-glucosidase from Pyrococcus furiosus and Agrobacterium faecalis share a common catalytic mechanism, *Biochemistry 37*, 17170−17178.
48. Li, Y. K., Chir, J., Tanaka, S., and Chen, F. Y. (2002) Identification of the general acid/base catalyst of a family 3 beta-glucosidase from *Flavobacterium meningosepticum*, *Biochemistry 41*, 2751−2759.
49. Tull, D., and Withers, S. G. (1994) Mechanisms of cellulases and xylanases: a detailed kinetic study of the exo-β-1,4-glycanase from *Cellulomonas fimi*, *Biochemistry 33*, 6363−6370.
50. Vocadlo, D. J., Wicki, K. R., and Withers, S. G. (2002) Mechanism of Thermoanaerobacterium saccharolyticum B-Xylosidase: Kinetic Studies, *Biochemistry 41*, 9727−9735.
51. Zechel, D. L., Reid, S. P., Stoll, D., Nashiru, O., Warren, R. A., and Withers, S. G. (2003) Mechanism, Mutagenesis, and Chemical Rescue of a β-Mannosidase from *Cellulomonas fimi*, *Biochemistry 42*, 7195−7204.
52. Wang, Q., Trimbur, D., Graham, R., Warren, R. A., and Withers, S. G. (1995) Identification of the acid/base catalyst in Agrobacterium faecalis β-glucosidase by kinetic analysis of mutants, *Biochemistry 34*, 14554−14562.
53. Jensen, J. L., and Jencks, W. P. (1979) Hydrolysis of benzaldehyde O,S-acetals, *J. Am. Chem. Soc. 101*, 1476−1488.
54. Ferraz, J. P., and Cordes, E. H. (1979) Kinetic α-secondary deuterium-isotope effects for O-ethyl S-phenyl benzaldehyde acetal hydrolysis, *J. Am. Chem. Soc. 101*, 1488−1491.
55. Fife, T. H., and Przystas, T. J. (1979) Intra-molecular general acid catalysis in the hydrolysis of acetals with aliphatic alcohol leaving groups, *J. Am. Chem. Soc. 101*, 1202−1210.
56. Burmeister, W. P., Cottaz, S., Driguez, H., Iori, R., Palmieri, S., and Henrissat, B. (1997) The crystal structures of Sinapis alba myrosinase and a covalent glycosyl-enzyme intermediate provide insights into the substrate recognition and active-site machinery of an S-glycosidase, *Structure 5*, 663−675.
57. Burmeister, W. P., Cottaz, S., Rollin, P., Vasella, A., and Henrissat, B. (2000) High-resolution X-ray crystallography shows that ascorbate is a cofactor for myrosinase and substitutes for the function of the catalytic base, *J. Biol. Chem. 275*, 39385−39393.
58. Porter, G. R., Rydon, H. N., and Schofield, J. A. (1958) Nature of the reactive serine residue in enzymes inhibited by organophosphorus compounds, *Nature 182*, 927−927.
59. Lowe, G., Sheppard, G., Sinnott, M. L., and Williams, A. (1967) Lysozyme-catalysed hydrolysis of some β-aryl di-*N*-acetylchitobiosides, *Biochem. J. 104*, 893−899.
60. Vocadlo, D. J., Davies, G. J., Laine, R., and Withers, S. G. (2001) Catalysis by hen egg-white lysozyme proceeds via a covalent intermediate, *Nature 412*, 835−838.
61. Haltiwanger, R. S., Grove, K., and Philipsberg, G. A. (1998) Modulation of O-linked *N*-acetylglucosamine levels on nuclear and cytoplasmic proteins in vivo using the peptide *O*-GlcNAc-β-*N*-acetylglucosaminidase inhibitor O-(2-acetamido-2-deoxy-D-glucopyranosylidene)amino-N-phenylcarbamate, *J. Biol. Chem. 273*, 3611−3617.
62. Clark, R. J., McDonough, P. M., Swanson, E., Trost, S. U., Suzuki, M., Fukuda, M., and Dillmann, W. H. (2003) Diabetes and the accompanying hyperglycemia impairs cardiomyocyte calcium cycling through increased nuclear *O*-GlcNAcylation, *J. Biol. Chem. 278*, 44230−44237.
63. Robinson, R. A., Davis, M. M., Paabo, M., and Bower, V. E. (1960) *Res. Nat. Bur. Stand. Sect. A 64*, 347−352.
64. Kortum, G., Vogel, W., and Andrussow, K. (1961) *Pure Appl. Chem. 1*, 187−536.
65. Barlin, G. B., and Perrin, D. D. (1966) Prediction of strengths of organic acids, *Q. Rev. 20*, 75−101.
66. Chenna, R., Sugawara, H., Koike, T., Lopez, R., Gibson, T. J., Higgins, D. G., and Thompson, J. D. (2003) Multiple sequence alignment with the Clustal series of programs, *Nucleic Acids Res. 31*, 3497−500.

BI052370B